metals

MDPI

Review

Quality Assessment of Laser Welding Dual Phase Steels

Eva S. V. Marques [1], António B. Pereira [1,2,*] and Francisco J. G. Silva [1,3,4]

[1] TEMA—Centre for Mechanical Technology and Automation, Department of Mechanical Engineering, Campus de Santiago, University of Aveiro, 3810-193 Aveiro, Portugal; eva.sv.marques@ua.pt (E.S.V.M.); fgs@isep.ipp.pt (F.J.G.S.)
[2] LASI—Intelligent Systems Associate Laboratory, 4800-058 Guimarães, Portugal
[3] INEGI—Instituto de Ciência e Inovação em Engenharia Mecânica e Engenharia Industrial, Rua Dr. Roberto Frias 400, 4200-465 Porto, Portugal
[4] ISEP—School of Engineering, Polytechnic of Porto, Rua Dr. António Bernardino de Almeida 431, 4200-072 Porto, Portugal
* Correspondence: abastos@ua.pt

Abstract: Since non-conforming parts create waste for industry, generating undesirable costs, it is necessary to set up quality plans that not only guarantee product conformity but also cut the root causes of welding defects by developing the concept of quality at origin. Due to their increasing use in automotive industry, dual phase (DP) steels have been the chosen material for this study. A quality plan for welding DP steel components by laser was developed. This plan is divided into three parts: pre-welding, during and post-welding. A quality assessment regarding mechanical properties, such as hardness, microstructure and tensile strength, was also performed. It was revealed that DP steel does not present considerable weldability problems, except for the usual softening of the heat affected zone (HAZ) and the growth of martensite in the fusion zone (FZ), and the best analysis techniques to avoid failures in these steels are finite element method (FEM), visual techniques during welding procedure and digital image correlation (DIC) for post-weld analysis.

Keywords: welding; laser welding; DP steels; welding quality; welding procedures; welding defects

Citation: Marques, E.S.V.; Pereira, A.B.; Silva, F.J.G. Quality Assessment of Laser Welding Dual Phase Steels. *Metals* **2022**, *12*, 1253. https://doi.org/10.3390/met12081253

Academic Editor: Xiangdong Gao

Received: 19 June 2022
Accepted: 24 July 2022
Published: 26 July 2022

1. Introduction

There are several international standards that industry must obey to guarantee quality on products obtained by welding processes. The entities responsible by issuing these standards are the following: EN (European Standards), ISO (International Organization for Standardization, Geneva, Switzerland), AWS (American Welding Society, Miami, FL, USA), ASME (American Society for Mechanical Engineers, New York, NY, USA), among others [1]. However, product quality does not depend exclusively on compliance with these standards, but also depends on other factors, such as the material itself, the welding conditions and the operator's experience, the last being the most critical. Nevertheless, in automated processes, defects can also occur due to incorrect parameter setting of the devices, lack of maintenance or failure of the system itself [2] (Figure 1).

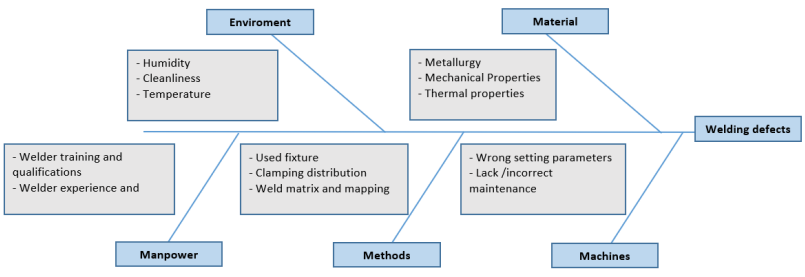

Figure 1. Ishikawa's diagram of welding defects.

Toivanen [3] refers that the criteria for producing welded joints are often unknown by most of the workers in a shop floor and by the hierarchy chain, which leads to constant non-conform products. It was concluded that the coordination of welding, according to ISO 3834 [4], is an asset for companies, as it contributes to the continuous improvement of the process and ensures quality requirements.

The ISO 6520 standard [5,6] describes some hypothetical defects that can occur in welded joints, especially in fusion or pressure welding processes. The standard defines that:

- "An imperfection in welding is the lack of continuity or deviation in the defined geometry";
- "A defect in welding is an inadmissible imperfection".

ISO 6520 defines the following as defects:

- Cracks;
- Cavities/porosities;
- Solid inclusions;
- Penetration failure;
- Dimensional defects;
- Various defects.

Within these defects, dimensional deviations or distortions are considered the most harmful for production, since they cause two main problems: firstly, it results in dimensional inaccuracies that make non-conform parts [7,8], and secondly, this defect increases production costs, due to the extra rework need to straighten the part, which, as reported in [9–14], is expensive in terms of time and ergonomics for workers.

Industries, such as automotive, aerospace and naval, are those that have higher costs about parts rectification. According to [15,16], the corrections of distortions reached 30% of the total cost of product manufacturing.

The industrial control of welding distortions is performed using empirical formulas, however, for larger and complex structures these formulas should not be applied [9]. The alternative is to use numerical models based on finite element analysis. The use of finite element analysis (FEA) requires an initial investment in equipment and is also time consuming [17]. Nevertheless, the time spent correcting the distortions is greater than the time spent performing the simulation. The use of these techniques had a significant contribution to the development of methods for the prevention of these defects [11].

Dual phase steels (DP) are one of the most studied steels in the automotive industry, especially after the 1990s when it was decided to reduce the cars' weight to reduce volatile organic compounds (VOC) and other emissions. These steels are composed by a ferritic matrix with about 5 to 20% martensite. The process of transforming austenite into martensite is done with intercritical heat treatment, followed by quenching [18,19]. Although the ductility tends to decrease with increasing stress [20], they have good mechanical characteristics with tensile stress values from 450 to 1200 MPa [18,21]. These steels are mainly used in the industry as stamped, but the need may arise from creating parts by welding. The spot welding process is one of the most used in the automotive industry, but the laser welding process has advantages, such as low heat input, low deformation after welding and high energy density [22].

The assessment regarding welding DP steel parts should be able to prevent defects from occurring, using finite element method (FEM) analysis to study the material behavior considering the parameterization used during the welding process. It is also necessary to control the possible occurrence of defects during the process, such as porosities, cracks, lack of penetration, etc., controlling the parameters of the welding fixture and ensuring that the operator follows procedures and standards. A batch sample should be subjected to some tests after production to check if there are any defects, such as dimensional errors or porosities in the bead.

2. Quality Assessment Pre-Welding: Virtual Prototype FEM Analysis

Due to advances in technology, it is now possible to prevent certain defects from occurring before starting the welding process. Indeed, there are defects that are possible to predict their behavior through numerical simulations, such as distortions and misalignment, as these defects are directly linked to the use of jigs and clamp placement (Table 1).

Table 1. How to prevent laser welding defects—pre-welding [23].

Problem	Potential Effects	Causes	Solutions	How to Prevent/ Control
Distortion and molten pool geometry	Geometric deformations	Welder inexperience	Welding resorting to jigs. Study and adjust jigs through simulation.	FEM analysis
		High heat input and number of beads.	Adjust welding parameters to reduce heat input and select the ideal quantity of beads.	
		Incorrect welding sequence	Study different welding sequencings through simulation.	
		Slow welding speed	Study different welding speeds in simulation.	

2.1. FEM Analysis

Simulation is a set of mathematical models or statistical tools, able to predict the behavior of a product when making specific inputs. Simulations can offer researchers the ability to impose certain conditions and obtain predictions about the results, which can be compared with experimental data. To exercise this comparison, it is necessary to choose an error percentage. There are several packages of software that can be used in this field, such as CAEplex, MATLAB, Ansys, OpenFOAM, EMS, SolidWorks Simulation Premium, COMSOL Multiphysics, Flow-3D, and ProModel Optimization Suite [24], among others.

To design a certain product, simulation plays a crucial role when it comes to execute a virtual prototype. This type of prototype will help to verify the ideal conditions under which the product must be manufactured. Regarding laser welding, it is possible to check the welding parameters and conditions, such as power, speed, weld bead size, operations sequencing, etc. Thus, the simulation allows the production of the product virtually to find possible unconformities before the prototype is physically executed, thereby eliminating costs of non-quality parts.

To perform a laser welding simulation of a DP steel regarding the study of strains and distortions that might occur during welding, it is necessary to implement thermo-mechanical simulation [25–27]. This type of simulation is highly used for studying large-sized structures, verifying if the residual stresses and distortions are contained within the tolerances. To perform this simulation requires three stages: thermal modelling, metallurgical modelling and mechanical modelling [28].

2.1.1. Thermal Model

For large structures, it is not yet possible to complete a full simulation (due to the amount of time required), thus, several assumptions are usually made about the interaction of the material with the process, which must be reduced to the volume of the heat source itself. This assumption generates difficulties, since gas and liquid flows are neglected. Therefore, it is necessary to include these effects in the volume of the heat source [28].

Heat transfer is an important phenomenon in the simulation, since the major consequences of the laser–material interaction are obtained by its thermal expansion [28]. To calculate this volume heat source, it is necessary to solve the equation for heat transfer

from the volumetric heat source to the metal during welding phase, considering convection and radiation heat losses [29]. Thus, some models can be chosen for simulating the heat source, such as Gaussian (conical heat source) and Goldak's model. [29].

2.1.2. Mechanical Model

In this field, two mechanical models can be used: the elastoplastic (EP) model and the elastoplastic with transformation induced volumetric strain model (VEP). The simulation of these two models can be carried out under the same conditions and meshing to verify different residual stress outputs. The resolution of the mechanical equation is based on the equation of static equilibrium, solving the global deformation during welding [30].

2.1.3. Metallurgical Model

During heating, the only transformation that occurs is into austenite, which does not depend completely on the heating rate [31]. Owing to changes in thermal expansion coefficient during the welding process, the phase transformation is a key step in modeling residual stresses [32]. This stage has two phases: thermal and mechanical. To carry out this simulation, it is necessary to consider variables, such as cooling rate, laser power and speed.

3. Quality Assessment during Welding

During the laser welding process, energy can be emitted in many ways, and to be able to study this energy and the effects that it will produce in the material, various methods can be used. Several use optical or acoustic sensors to be able to have a physical model of the phenomena, which occurs between laser and material, including defects that may happen during the laser welding process (Figure 2) [33].

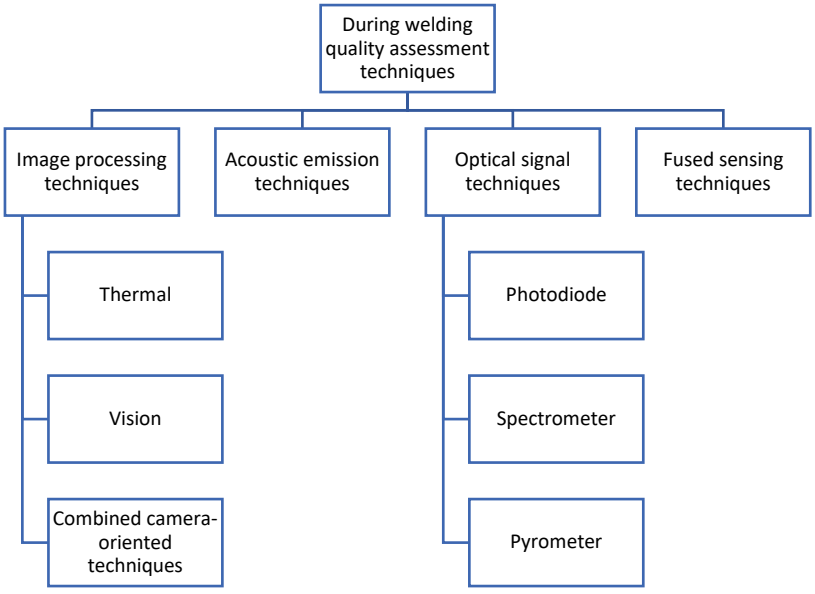

Figure 2. Quality assessment during welding [34].

In the literature, [34] shows that nowadays it is possible to control laser welding in real time and evaluate defects that might occur during the welding process, such as blow-outs, undercuts and lack of penetration (Table 2).

Table 2. How to prevent laser welding defects—during welding [23].

Problem	Potential Effects	Cause	Solution	How to Prevent/ Control
Blowout	The bead section can be weakened, affecting the mechanical strength of the joint.	Human failure	Hire highly skilled welders with certification.	Thermal
		Low welding current	Increase welding current	
		High speed	Lower welding speed	
Lack of penetration	Weakening of the bead section, stress concentrations, nucleation of cracks, which can lead to joint collapse.	Low pre-heating	Increase pre-heating temperature	Thermal Combined Acoustic emission techniques Photodiode sensor Pyrometer sensor
		High welding speed	Decrease welding speed	
		Human failure	Hire highly skilled welders with certification.	
Undercut	Reduction in the part's resistance when it is in working cycle.	High heat input in the joint.	Decrease welding power and adjust welding speed.	Thermal Vision Combined Photodiode sensor Fused techniques
Porosity	Decrease in resistance of the welding bead	Human failure	Hire highly skilled welders with certification.	Thermal
		Excessive flow rate in the shielding gas	Control shielding gas flow	
		Inclusion of oxygen due to ineffective gas protection	Remove impurities and follow standards for joint preparation.	
		High welding speed.	Decrease welding speed.	

In the column "How to prevent/control", several techniques have been presented, which are explained in the next section:

3.1. Image Processing Techniques

These techniques focus on extracting information, patterns and features from a set of images. They are used in various types of welding, including laser welding. They are divided into three categories:

- Thermal: this method studies the thermal field. IR thermal cameras can be used to capture the temperature distribution in the part to be welded. It is expensive and low sampling [35–38].
- Vision: with this method it is possible to characterize plasma plume, spatters and molten pool in welding. In the literature, there are papers in which a vision system was used together with vision sensor, based on the principle of triangulation in which it is possible to obtain information through 3D profiles. Some authors also used couple charged device (CCD) sensors to extract surface information, such as depth pool [39–41].
- Combined camera-oriented techniques: it is possible to check molten pool, thermal field, spatters and plasma plume. Since CCD cannot detect mid and long infrared

radiations, this technique joints thermal IR cameras with CCD sensor. It is expensive and presents setup limitations [42–44].

3.2. Acoustic Emission Techniques

With this technique, it is only possible to study the plume vapor and the workpiece. The only defect that can be verified is penetration, but since this system is very dependent on sound waves, it has the disadvantage that it is very sensitive to sound [45–47].

3.3. Optical Techniques

These techniques are used essentially for monitoring the welding process itself. The optical sensors are classified in the following three categories:

- Photodiode sensor: the variables that can be characterized are steam plume, thermal radiation and reflected laser beam energy. This method is not able to detect microdefects, but its low cost is an advantage [48–50];
- Spectrometer: only able to check the spectrum of plasma plume and spatters. The only limitation is that they can only check the behavior of the plume [51,52];
- Pyrometer sensor: it detects changes in temperature by thermal radiation. It is used to characterize the molten pool and steam plume. It can be used for real-time temperature monitoring and online quality control [53–55].

3.4. Fused Techniques

Fused techniques are a new belief that a multi-sensor approach can be more accurate in obtaining data from welding processes, which will improve the study of welding defects. Authors have studied combinations of infrared and ultraviolet sensors with acoustic techniques and visual sensing with photodiode sensing [56–58].

4. Quality Assessment Post-Welding

Even with all existing standards, there is always room for error (Figure 3). Therefore, after the laser welding process, a sample of parts should be taken and submitted to tests to verify if the batch complies to the requirements.

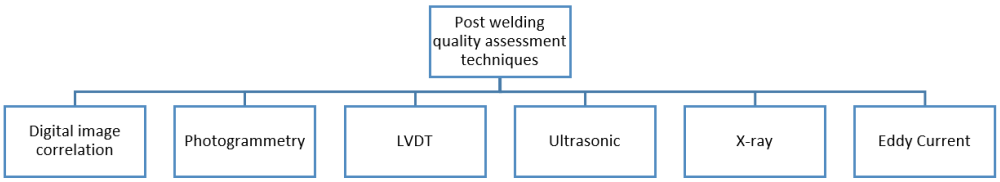

Figure 3. Quality assessment post-welding [34].

Each technique presented in Figure 3 is explained in the following section.

4.1. Digital Image Correlation (DIC)

The digital image correlation (DIC) concept used by [59–61] is a method of optical analysis, without contact and of total field. With the use of two cameras and image recording techniques, using correlation algorithms, the surfaces and the outline of an object can be determined using the DIC method. The surface profiles obtained before and after welding are compared with the results of the 3D deformation of the object. This method requires the proper calibration of the cameras and can be used to measure any type of transient welding distortion, as well as welding distortion after the process. The DIC software, ARAMIS®, developed by GOM©, is one of the best known in this field.

4.2. Photogrammetry

This is a method based on remote sensors that uses photographs to get the exact place of a point or surface using the triangulation of several points. To measure the distortion occurred in the welding process, the most used type is short-range photogrammetry. In this method, the camera is close to the object. The configuration used in photogrammetry is like that of DIC and can be used to obtain the 3D models of the photographed object [62].

4.3. Linear Variable Differential Transformer (LVDT)

Another method that can be used is LVDT, which is a device like an electrical transformer that measures linear displacements, measuring the variation of the induced internal voltage. The LVDT can be used to measure the size of the distortion at fixed points during welding and after cooling it [63,64].

4.4. Ultrasonic

Ultrasonic inspection methods involve the generation of ultrasonic waves that interact with the weld. If there are defects in the bead, these will cause waves to be reflected and diffracted. Within the ultrasonic waves, a technique called time of flight measurement (ToF) allows calculating the quality of the bead through its geometry. However, to apply this method, an exact knowledge of the speed of sound is necessary to define the geometry [65–67].

4.5. X-ray Radiography

X-rays and gamma rays can be used to show discontinuities and inclusions within opaque material. This feature has become useful in the study of weld beads, where it is possible to verify defects, such as porosities. However, this technique requires the operator to be qualified in interpreting the results. Moreover, it is very expensive due to the handling of parts, equipment and the necessary protection. Usually, it is not used in automated environments [68–72].

4.6. Eddy Current

Defects and changes in material properties result in changes in the signals of these currents. This method has a great ability to detect distinctive defects in welds with a depth of less than 2 mm, and it can be automated in the inspection after the welding process. Despite the advantages, it is only applicable to conductive materials. However, the surface of the welds must be accessible to the probe because the surface finish and its irregularities can interfere with the reference standard [73–76].

4.7. Magneto-Optical Detection Method

This procedure is a non-destructive testing based on magneto-optical (MO) imaging, which transforms the magnetic leakage field into a light intensity map to visualize defects [77–79]. In the study [80], a vertical combined magnetic field (VCNF) and a parallel combined magnetic field (PCMF) were compared to traditional magnetic fields where it was found that magneto-optical imaging under VCMF could detect weld defects of any shape and distribution accurately. This technique was also used in [81], where weld surface and subsurface cracks were detected by an MO sensor. It was shown that the magnetic flux leakage signals of the weld surface and subsurface cracks could be easily distinguished.

5. Quality Assessment Considering Mechanical Properties

In laser welding, the most common welding joint is butt welding. In this type of joint, it is necessary to pay special attention to the alignment of the parts, as the size beam is very narrow compared to other fusion welding processes. Any space between the parts to

be joined will cause defects, such as weld concavity, undercut, and the appearance of a notch that increases fatigue in parts [82].

In industry, the laser welding process with keyhole is used, due to the high penetration and fast welding speed, but it can cause defects, such as rough and ropy surfaces due to the instability of the keyhole. In addition to these problems, there are also metallurgical problems, such as the softening of the HAZ. This phenomenon occurs because the martensite present in DP steel is tempered [82]. This problem will be described in the following Section 5.1.

5.1. Hardness

Gathering several authors, it was possible to conclude that there are two main problems regarding hardness in DP laser welding joints: the growth of martensite in fusion zone (FZ), and a softening phenomenon in the HAZ.

1. Growth of martensite in FZ:
    - The amount of martensite contributes to the decrease of the joint ductility, as demonstrated in [83]. For example, the welding parameters presented in [84] led to a 53.7% increase in hardness in the fusion zone.
    - It was possible to conclude in [85] that hardness in FZ, duplicated its original value, due to the rapid cooling rate after the welding process.
    - The higher the welding speed, the higher the cooling rate [82,86].
    - The FZ is strongly dependent on the carbon content. It was verified by [82] that FZ decreased with the increasing of carbon and other alloys.

Table 3 represents an outline of the papers where the hardness of laser welded DP steels was studied. It can be verified that hardness in FZ is always greater than in HAZ, due to the existence of martensite in FZ.

Table 3. Hardness values for several laser welded DP steels.

Author	Material	Welding Method/Power (W)	Laser Type	Hardness FZ (HV)	Hardness HAZ (HV)
Xie et al. [81]	DP590	Continuous/3000	Fiber	365	180
Sun et al. [87]	DP590	Pulsed/132	Nd:YAG	270	160
Mansur et al. [88]	DP600	Continuous/1200–1500	Fiber	350	200
Tuncel et al. [89]	DP600	Pulsed/300	Nd:YAG	300–400	200–400
Gandhi et al. [90]	DP780	Pulsed/325	Nd:YAG	385	240
Huang et al. [91]	DP980	Continuous/1000–2000	Fiber	500	325
Jia et al. [92]	DP980	Continuous/4000	Fiber	415	320
Parkes et al. [93]	DP980	Continuous/6000	Fiber	410	240
Saha et al. [94]	DP980	Continuous/6000	Fiber	480	295
Xu et al. [95]	DP980	Continuous/6000	Fiber	480	280
Tuncel et al. [89]	DP1000	Pulsed/300	Nd:YAG	350–400	290–360

2. Softening phenomenon in HAZ:
    - HAZ softening has been associated with tempered martensite in the base metal.
    - The width of soft zone decreases with increasing welding speed and decreasing beam width.

- It was also found in [96] that the appearance of fine-grained martensite in the subcritical HAZ results in an increased hardness, while the tempered martensite contributes to a soft zone.
- The size of the HAZ soft zone decreased with increasing pulse duration 83.
- In the work of [97], DP600, DP800 and DP1000 were studied, verifying that HAZ softening increased with steel grades, which is related to the amount of martensite in each type of DP steel.

To deal with the appearance of martensite and its contribution to increasing hardness, it is possible to use thermal treatments: post-welding heat treatment (PWHT) and pre heat welding treatment (PHWT).

1. Pre Heat Welding Treatment:
   - In [98], the study of DP980 steel welded at room temperature and preheated to 526 °C has been performed. Using preheating, it was observed that the microstructure in the FZ of the bead changed from martensitic (with a hardness between 320 and 500 HV) to a microstructure composed by bainite, ferrite and austenite, presenting 280 HV of hardness.
2. Post-Welding Heat Treatment:
   - In paper [85], two types of thermal treatments were tested with the purpose of resetting the initial characteristics of DP600 before welding. The hardness values in the welding and in the HAZ dropped significantly but still showed values 40% above the base metal. In paper [99], PWHT has been used in a DP1400 steel, and it was shown that the heat treatment had little significance regarding tensile strength due to the transformation of martensite into tempered martensite. However, it had relevant results with elongation, which contributes to lower defects, such as cold cracking.
   - In the paper presented by [100], it was verified that using post-welding heat treatments, the tensile stress decreased from 725 ± 7 MPa to 679 ± 5 MPa, but the elongation increased from 2.8% to 3.5%.

5.2. Microstructure

In addition to the nomenclature used to characterize welding joints, BM (base metal), FZ (fusion zone), HAZ (heat affected zone), there is an extra nomenclature that was adopted for the HAZ [99–101]. In steels, the peak temperature achieved in the HAZ results in specific metallurgical transformations is based on the local phase diagram (Figure 4). The main transformations in DP steels are described below:

1. Sub-critical HAZ (S-HAZ) is the region where the peak temperature during welding is below Ac_1 temperature of steel phase diagram [101].
   - It was verified by [101] that martensite in the BM was transformed into tempered martensite during subsequent heating and cooling, since the local temperature was below Ac_1 and austenization did not take place.
   - The martensite phase in the BM is tempered causing HAZ to soften. The severity of HAZ softening decreases with increasing distance from the Ac_1 isotherm [82].
2. Inter-critical HAZ (I-HAZ) is the region where the peak temperature during welding is between Ac_1 and Ac_3 temperature of steel phase diagram [101].
   - It was verified by [101] that the local peak temperature was between Ac_3 and Ac_1; originating the austenitization of martensite and ferrite from BM and after cooling, it transformed into ferrite and M-A constituent.
   - The volume fraction of martensite in the HAZ increases as the peak temperature rises from Ac_1 to Ac_3 [82].
3. Super-critical or upper-critical HAZ (SC-HAZ): during welding, the steel is heated above Ac_3 [101].

- The microstructure changes to austenite during heating. Depending on how high above Ac_3 the temperature is, it can also occur grain growth. When the area of the HAZ with a temperature above Ac_3 cools down, it transforms into martensite [82].

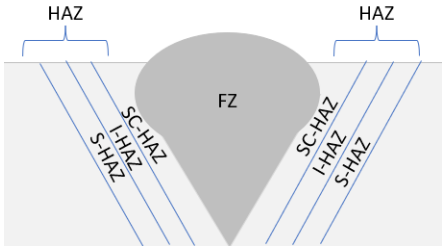

Figure 4. HAZ areas [102].

Table 4 shows a summary of papers with all microstructures that were originated by laser welding in several DP steels in the HAZ.

Table 4. Microstructural transformations in HAZ.

Author	Material	Welding Method/Power (W)	S-HAZ	I-HAZ	SC-HAZ
Sun et al. [87] —single spot	DP590	Pulsed/132	TM + F	M + F	LM
Sun et al. [87] —8 (pulse)	DP590	Pulsed/132	TM + TB	LM + B + M-A	LM
Di et al. [101]	DP780	Continuous/2000	TM	F + M-A	LM
Parkes et al. [93]	DP980	Continuous/6000	PTM	M	TM
Saha et al. [94]	DP980	Continuous/6000	-	F + M + Carbides	M + B

TM—tempered martensite/F—ferrite/TB—tempered bainite/PTM—partial tempered martensite/M—martensite/LM—lath martensite/M-A—martensite–austenite compound.

It is possible to verify the existence of predominant structures as: TM in S-HAZ, Martensite and Ferrite in I-HAZ and LM in SC-HAZ, in almost all grades of DP steel.

Effects of Laser Characteristics in Microstructure

Heat input is the ratio between laser power and welding speed; it increases with laser power and decreases with welding speed [102]. Heat input not only affects softening phenomenon but also the appearance of defects, such as lack of penetration and pores. The effect of heat input is usually detrimental for the mechanical properties of welded joint [86].

- Heat input too low (excessive welding speed or insufficient power) may cause lack of penetration and pores at FZ in the welded joint [79,103].
- Heat input too high generates larger weld beads, promotes HAZ softening and leads to a less refined microstructure [104].
- Lower speed favours weld penetration but increase heat dissipation in the transverse direction to weld, which leads to wider welds.
- Constant welding speed increases welding width and penetration [103].

5.3. Tensile Properties

Metallurgical properties have a direct influence on the tensile and yield strength values of all DP steels. The softening phenomenon, for example, can contribute to the collapse of the joint in the HAZ. Table 5 shows the results obtained in the studies regarding the mechanical properties of the welded joints of various types of DP steels.

Table 5. Mechanical properties of DP steels weld joints.

Author	Material	Welding Method/Power	Yield Strength Re MPa	Ultimate Tensile Strength UTS MPA	Total Elongation %
Mansur et al. [88]	DP600	Continuous/1200–1500	363 *	629 *	15.7
Di et al. [101]	DP780	Continuous/2000	525	875	17.2
He et al. [105]	DP800	Continuous/3000	701	868	7.9
Di et al. [101]	DP980	Continuous/2000	695	1080	12.7
Parkes et al. [93]	DP980	Continuous/6000	720	1067	5.3
Saha et al. [94]	DP980	Continuous/6000	725	1041	4.7
He et al. [105]	DP1000	Continuous/3000	883	1034	1.9

* Average values.

It was verified in [88] that the welding process did not change the component yield behavior. All samples reached the minimum required UTS for DP600 (600 MPa). All samples have broken at BM, which confirms the absence of softening phenomenon.

Regarding DP780 [101], the fracture occurred in BM. In the fracture surface, dimples were observed, which means ductile fracture. The curves of similar welding joints were like BM ones. In that study, high welding speed and lower heat input was selected, thus, HAZ softening did not occur.

It was found in [105] that different thicknesses (1.3 to 2.1 mm), for the DP800 joints, did not significantly affect the strength properties, and the fracture occurred in the BM. In DP1000 steel, the elongation at fracture was reduced compared to the BM values, and the fracture arose at the welded joint.

Regarding fiber laser [93], the strength of welded joints did not decrease in contrast to welded joints made with diode laser. It was possible to verify the existence of a smaller soft zone in the joints produced by fiber laser, than in the joints made by diode laser. It can be concluded that a smaller laser beam spot, together with a higher power and speed in the fiber laser, significantly increased the joint strength by decreasing the soft zone.

It was found in [94], that increasing the welding speed from 12 m/min to 16 m/min, resulted in a decrease in UTS from 1081 MPa to 1041 MPa, although YS has remained like BM. Fracture occurred in SC-HAZ due to low hardness values (softening phenomenon).

In this work, welded joints on different energy inputs were studied (325 J/mm and 108 J/mm), observing that a low energy input has resulted in greater ductility and, consequently, greater elongation.

6. Discussion

Of all these techniques under analysis in this paper, it is necessary to verify their effectiveness if they will be more appropriate to the industrial or laboratory scope, regarding the research purposes. To study DP steel, a finite element analysis is necessary, where a study of influence of laser welding process in the thermal field is verified. Therefore, the most appropriate analysis techniques to carry out during welding (both laboratory and industrial) are visual techniques. Among them, the most favorable will be the combination

of the thermal with the visual ones, due to the variables that are possible to quantify (including the thermal field) and the possible defects to be observed. However, in this case, the high costs for the use of this technique can only be justified due to the necessary investigation around this material. Moreover, at the industrial level, the same costs can be amortized in the production of the parts.

Regarding post-weld analysis for laboratory methods, any of the techniques are reliable, although laboratories should have the necessary resources to execute these methods. If the case is transposed to the industrial field, it is possible to conclude that the ultrasonic method is not practical, this method only works below the surface and only from 2–3 mm, which in a 3 mm DP plate it is not possible to evaluate anything. Additionally, it is difficult to obtain X-ray equipment, so this method is also discarded at industry level. The best option is to opt for DIC or photogrammetry techniques, where it essentially involves the acquisition of equipment that, as in the case of vision techniques, can be amortized in the production of components. Table 6 exhibits a summary of which techniques can be used in industry or in the laboratory field.

Table 6. Comparison of techniques (Industrial vs. Laboratory).

Technique	Industry	Laboratory
FEM analysis	X	X
Thermal	X	X
Vision	X	X
Combined		X
Acoustic emission techniques		X
Photodiode	X	X
Spectrometer	X	X
Pyrometer	X	X
Fused Techniques		X
DIC	X	X
Photogrammetry	X	X
LVDT	X	X
Ultrasonic		X
X-ray		X
Eddy current	X	X
Hardness tests		X
Metallographic tests		X
Tensile tests		X

In the industrial field, it is not easy most of the time to perform metallographic analysis, which would be necessary to resort to a laboratory. Therefore, analysis must be carried out in specific cases to try to discover if the root cause of a certain defect, has its origin in a phase transformation.

The main defects in DP steels are the appearance of martensite in the FZ and the phenomenon of softening in the HAZ of the joint. To overcome these defects, heat treatments should be used. Thus, the company must carry out energy cost studies to verify the cost–benefit results, and whether to buy ovens to carry out these treatments or to subcontract them.

Tensile tests of laser welded DP steel specimens must be performed before this steel is used for production. The welds must be performed by the welder responsible for the process, with the parameters defined by the FEM analysis, to verify that the mechanical properties of the bead are within the values presented in Table 5.

The values obtained in Tables 3–5 can be used as reference values for welded joints of various grades of DP steel, although the hardness values (Table 3) can always be improved using heat treatments. The metallographic values can also be studied for different laser types, laser modes and other parameters, such as speed and power. From there it would be possible to have a standard for all DP steel grades. The values presented in Table 5 can be used as UTS values for the presented grades of DP steel, since for all of them, a UTS above the standard of the raw material was achieved.

Regarding sequence, tensile tests should be done pre-welding, metallography and hardness post-welding.

To study more acceptance criteria for welding quality, the following standards can be employed: 3834-1 [106], ISO. 3834-2 [107], ISO. 3834-4 [108], ISO. 3834-5 [109], ISO. 9001 [110], DIN. 18800-7:2008 [111] and ISO. 15609-4:2009 [112].

7. Conclusions

DP steels and laser welding are increasingly being studied, due to their environmental impact on the automotive industry.

In this paper, a theoretical study about the quality criteria in laser welding DP steels is presented. The quality assessment for these steels was developed regarding general aspects of laser welding and specific criteria for DP steels due to their chemical composition and specific mechanical properties and microstructure.

DP steel does not present considerable weldability problems, except for the usual softening of the HAZ and the growth of martensite in the FZ, which can increase hardness in the weld bead.

The best analysis techniques to avoid failures in DP steel are FEM, visual techniques during welding procedure and DIC for post-weld analysis.

This plan is divided into three stages related to the welding process: pre, during and post welding. The values exposed in Tables 4–6 should be considered as possible references for welded joints for the different DP steels grades. This plan was developed considering a possible application in industry, helping researchers rapidly understand what kind of values they can expect in their works as well.

Author Contributions: E.S.V.M.: investigation and writing original draft; F.J.G.S.: conceptualization, supervision, writing—review and editing; A.B.P.: supervision, writing—review and editing. All authors have read and agreed to the published version of the manuscript.

Funding: The present work was done and funded under the scope of projects UIDB/00481/2020 and UIDP/00481/2020—FCT—Fundação para a Ciencia e a Tecnologia; and CENTRO-01-0145-FEDER-022083—Centro Portugal Regional Operational Programme (Centro2020), under the PORTUGAL 2020 Partnership Agreement, through the European Regional Development Fund. LAETA/INEGI/CETRIB is acknowledge due to the support provided in all research activities.

Institutional Review Board Statement: Not applicable.

Informed Consent Statement: Not applicable.

Data Availability Statement: Not applicable.

Conflicts of Interest: The authors declare no conflict of interests regarding this paper.

References

1. Pereira, A.B.; de Melo, F.J.M.Q. Quality Assessment and Process Management of Welded Joints in Metal Construction—A Review. *Metals* **2020**, *10*, 115. https://doi.org/10.3390/met10010115.
2. *DIN. V 4113-3:2003;* Aluminium Constructions under Predominantly Static Loading—Part 3: Execution and Qualification of Constructors. German Institute for Standardization: Berlin, Germany, 2003.
3. Toivanen, J.; Kah, P.; Martikainen, J. Quality Requirements and Conformity of Welded Products in the Manufacturing Chain in Welding Network. *Int. J. Mech. Eng. Appl.* **2015**, *3*, 109. https://doi.org/10.11648/j.ijmea.20150306.12.
4. *ISO 3834-3:2005*; Quality Requirements for Fusion Welding of Metallic Materials—Part 3: Standard Quality Requirements. International Organization for Standardization: Geneva, Switzerland, 2005.

5. *ISO 6520-2:2013*; Welding and Allied Processes—Classification of Geometric Imperfections in Metallic Materials, Part 2 Weld. International Organization for Standardization: Geneva, Switzerland, 2013.
6. *ISO 6520-1:2007*; Welding and Allied Processes—Classification of Geometric Imperfections in Metallic Materials, Part 1 Fusion Welding. International Organization for Standardization: Geneva, Switzerland, 2007.
7. Camilleri, D.; McPherson, N.; Gray, T.G. The applicability of using low transformation temperature welding wire to minimize unwanted residual stresses and distortions. *Int. J. Press. Vessel. Pip.* **2013**, *110*, 2–8. https://doi.org/10.1016/j.ijpvp.2013.04.014.
8. Deng, D.; Murakawa, H.; Liang, W. Numerical simulation of welding distortion in large structures. *Comput. Methods Appl. Mech. Eng.* **2007**, *196*, 4613–4627. https://doi.org/10.1016/j.cma.2007.05.023.
9. Bachorski, A.; Painter, M.; Smailes, A.; Wahab, M. Finite-element prediction of distortion during gas metal arc welding using the shrinkage volume approach. *J. Mater. Process. Technol.* **1999**, *92–93*, 405–409. https://doi.org/10.1016/s0924-0136(99)00161-2.
10. Ghosh, B.P.K.; Devakumaran, K.P. Effect of Pulse Current on Shrinkage Stress and Distortion in Multipass GMA Welds of Different Groove Sizes. *AWS* **2010**, *89*, 43–53.
11. Choobi, M.S.; Haghpanahi, M.; Sedighi, M. Prediction of welding-induced angular distortions in thin butt-welded plates using artificial neural networks. *Comput. Mater. Sci.* **2012**, *62*, 152–159. https://doi.org/10.1016/j.commatsci.2012.05.032.
12. Wang, J.; Shibahara, M.; Zhang, X.; Murakawa, H. Investigation on twisting distortion of thin plate stiffened structure under welding. *J. Mater. Process. Technol.* **2012**, *212*, 1705–1715. https://doi.org/10.1016/j.jmatprotec.2012.03.015.
13. Tian, L.; Luo, Y.; Wang, Y.; Wu, X. Prediction of transverse and angular distortions of gas tungsten arc bead-on-plate welding using artificial neural network. *Mater. Des.* **2014**, *54*, 458–472. https://doi.org/10.1016/j.matdes.2013.08.082.
14. Deng, D.; Zhou, Y.; Bi, T.; Liu, X. Experimental and numerical investigations of welding distortion induced by CO2 gas arc welding in thin-plate bead-on joints. *Mater. Des.* **2013**, *52*, 720–729. https://doi.org/10.1016/j.matdes.2013.06.013.
15. Holder, R.; Larkin, N.; Li, H.; Kuzmikova, L.; Pan, Z.; Norrish, J. Development of a DC-LSND welding process for GMAW on DH-36 Steel. In Proceedings of the 56th WTIA annual conference 2011, Cairns, Queensland, Australia, 25–27 September 2011; pp. 1–13.
16. Shen, C. Low Distortion Welding for Shipbuilding Industry. Master's Thesis, University of Wollongong, Kowloon City, Hong Kong, 2013.
17. Deng, D.; Murakawa, H. FEM prediction of buckling distortion induced by welding in thin plate panel structures. *Comput. Mater. Sci.* **2008**, *43*, 591–607. https://doi.org/10.1016/j.commatsci.2008.01.003.
18. Gomes, T.; Silva, F.; Campilho, R. Reducing the Simulation Cost on Dual-phase Steel Stamping Process. *Procedia Manuf.* **2017**, *11*, 474–481. https://doi.org/10.1016/j.promfg.2017.07.138.
19. Regueras, J.M.G.; López, A.M.C. Investigations on the influence of blank thickness (t) and length/wide punch ratio (LD) in rectangular deep drawing of dual-phase steels. *Comput. Mater. Sci.* **2014**, *91*, 134–145. https://doi.org/10.1016/j.commatsci.2014.04.024.
20. Tisza, M.; Lukács, Z. Springback Analysis of High Strength Dual-phase Steels. *Procedia Eng.* **2014**, *81*, 975–980. https://doi.org/10.1016/j.proeng.2014.10.127.
21. Fonstein, N. *Advanced High Strength Sheet Steels*, 1st ed.; Springer: Cham, Switzerland, 2015.
22. Xue, X.; Pereira, A.; Vincze, G.; Wu, X.; Liao, J. Interfacial Characteristics of Dissimilar Ti6Al4V/AA6060 Lap Joint by Pulsed Nd:YAG Laser Welding. *Metals* **2019**, *9*, 71. https://doi.org/10.3390/met9010071.
23. Silva, F.J.G. *Tecnologia da Soldadura Uma Abordagem Técnico-Didática*, 2nd ed.; Quântica Editora: Porto, Portugal, 2016; ISBN 9789897231704. (In Portuguese).
24. Butt, J. A Strategic Roadmap for the Manufacturing Industry to Implement Industry 4.0. *Designs* **2020**, *4*, 11. https://doi.org/10.3390/designs4020011.
25. Martinson, P.; Daneshpour, S.; Koçak, M.; Riekehr, S.; Staron, P. Residual stress analysis of laser spot welding of steel sheets. *Mater. Des.* **2009**, *30*, 3351–3359. https://doi.org/10.1016/j.matdes.2009.03.041.
26. Zain-ul-Abdein, M.; Nelias, D.; Jullien, J.F.; Deloison, D. Prediction of laser beam welding-induced distortions and residual stresses by numerical simulation for aeronautic application. *Mater. Process. Technol.* **2009**, *209*, 2907–2917.
27. Zain-Ul-Abdein, M.; Nélias, D.; Jullien, J.-F.; Boitout, F.; Dischert, L.; Noe, X. Finite element analysis of metallurgical phase transformations in AA 6056-T4 and their effects upon the residual stress and distortion states of a laser welded T-joint. *Int. J. Press. Vessel. Pip.* **2011**, *88*, 45–56. https://doi.org/10.1016/j.ijpvp.2010.10.008.
28. Dal, M.; Fabbro, R. An overview of the state of art in laser welding simulation. *Opt. Laser Technol.* **2016**, *78*, 2–14. https://doi.org/10.1016/j.optlastec.2015.09.015.
29. Kouadri-Henni, A.; Seang, C.; Malard, B.; Klosek, V. Residual stresses induced by laser welding process in the case of a dual-phase steel DP600: Simulation and experimental approaches. *Mater. Des.* **2017**, *123*, 89–102. https://doi.org/10.1016/j.matdes.2017.03.022.
30. Bonollo, P.F.H.P.A.T.F. The influence of phase transformations on residual stresses induced by the welding process—3d and 2d numerical models. *Model. Simul. Mater. Sci. Eng.* **2006**, *14*, 117–136.
31. Leblond, J.; Devaux, J. A new kinetic model for anisothermal metallurgical transformations in steels including effect of austenite grain size. *Acta Met.* **1984**, *32*, 137–146. https://doi.org/10.1016/0001-6160(84)90211-6.
32. Deng, D. FEM prediction of welding residual stress and distortion in carbon steel considering phase transformation effects. *Mater. Des.* **2009**, *30*, 359–366. https://doi.org/10.1016/j.matdes.2008.04.052.

33. Shao, J.; Yan, Y. Review of techniques for on-line monitoring and inspection of laser welding. *J. Phys. Conf. Ser.* **2005**, *15*, 101–107. https://doi.org/10.1088/1742-6596/15/1/017.
34. Stavridis, J.; Papacharalampopoulos, A.; Stavropoulos, P. Quality assessment in laser welding: A critical review. *Int. J. Adv. Manuf. Technol.* **2017**, *94*, 1825–1847. https://doi.org/10.1007/s00170-017-0461-4.
35. Chen, Z.; Gao, X. Detection of weld pool width using infrared imaging during high-power fiber laser welding of type 304 austenitic stainless steel. *Int. J. Adv. Manuf. Technol.* **2014**, *74*, 1247–1254. https://doi.org/10.1007/s00170-014-6081-3.
36. Speka, M.; Matteï, S.; Pilloz, M.; Ilie, M. The infrared thermography control of the laser welding of amorphous polymers. *NDT E Int.* **2008**, *41*, 178–183. https://doi.org/10.1016/j.ndteint.2007.10.005.
37. Bardin, F.; Morgan, S.; Williams, S.; McBride, R.; Moore, A.J.; Jones, J.D.C.; Hand, D.P. Process control of laser conduction welding by thermal imaging measurement with a color camera. *Appl. Opt.* **2005**, *44*, 6841–6848. https://doi.org/10.1364/ao.44.006841.
38. Hutter, F.X.; Brosch, D.; Graf, H.-G.; Klingler, W.; Strobel, M.; Burghartz, J.N. A 0.25 μm logarithmic cmos imager for emissivity-compensated thermography. In Proceedings of the 2009 IEEE International Solid-State Circuits Conference-Digest of Technical Papers, San Francisco, CA, USA, 8–12 February 2009; pp. 354–355.
39. Saeed, G.; Zhang, Y.M. Weld pool surface depth measurement using a calibrated camera and structured light. *Meas. Sci. Technol.* **2007**, *18*, 2570–2578. https://doi.org/10.1088/0957-0233/18/8/033.
40. Huang, W.; Kovacevic, R. A Laser-Based Vision System for Weld Quality Inspection. *Sensors* **2011**, *11*, 506–521. https://doi.org/10.3390/s110100506.
41. Zhang, Y.; Gao, X. Analysis of characteristics of molten pool using cast shadow during high-power disk laser welding. *Int. J. Adv. Manuf. Technol.* **2013**, *70*, 1979–1988. https://doi.org/10.1007/s00170-013-5442-7.
42. Al-Habaibeh, A.; Shi, F.; Brown, N.; Kerr, D.; Jackson, M.; Parkin, R.M. A novel approach for quality control system using sensor fusion of infrared and visual image processing for laser sealing of food containers. *Meas. Sci. Technol.* **2004**, *15*, 1995–2000. https://doi.org/10.1088/0957-0233/15/10/008.
43. von Witzendorff, P.; Kaierle, S.; Suttmann, O.; Overmeyer, L. Using pulse shaping to control temporal strain development and solidification cracking in pulsed laser welding of 6082 aluminum alloys. *J. Mater. Process. Technol.* **2015**, *225*, 162–169. https://doi.org/10.1016/j.jmatprotec.2015.06.007.
44. Voelkel, D.D.; Mazumder, J. Visualization of a laser melt pool. *Appl. Opt.* **1990**, *29*, 1718–1720.
45. Dorsch, F.; Braun, H.; Keßler, S.; Magg, W.; Pfitzner, D.; Plaßwich, S. Process Sensor Systems for Laser Beam Welding: Enabling and assuring reliable production. *Laser Tech. J.* **2012**, *9*, 24–28.
46. Li, L. A comparative study of ultrasound emission characteristics in laser processing. *Appl. Surf. Sci.* **2001**, *186*, 604–610. https://doi.org/10.1016/s0169-4332(01)00695-x.
47. Purtonen, T.; Kalliosaari, A.; Salminen, A. Monitoring and Adaptive Control of Laser Processes. *Phys. Procedia* **2014**, *56*, 1218–1231. https://doi.org/10.1016/j.phpro.2014.08.038.
48. Park, Y.W.; Park, H.; Rhee, S.; Kang, M. Real time estimation of CO2 laser weld quality for automotive industry. *Opt. Laser Technol.* **2002**, *34*, 135–142. https://doi.org/10.1016/s0030-3992(01)00103-7.
49. You, D.; Gao, X.; Katayama, S. Multiple-optics sensing of high-brightness disk laser welding process. *NDT E Int.* **2013**, *60*, 32–39. https://doi.org/10.1016/j.ndteint.2013.07.005.
50. Zhang, X.; Chen, W.; Ashida, E.; Matsuda, F. Relationship between weld quality and optical emissions in underwater Nd: YAG laser welding. *Opt. Lasers Eng.* **2004**, *41*, 717–730. https://doi.org/10.1016/s0143-8166(03)00031-9.
51. Rizzi, D.; Sibillano, T.; Calabrese, P.P.; Ancona, A.; Lugarà, P.M. Spectroscopic, energetic and metallographic investigations of the laser lap welding of AISI 304 using the response surface methodology. *Opt. Lasers Eng.* **2011**, *49*, 892–898. https://doi.org/10.1016/j.optlaseng.2011.02.014.
52. Sebestova, H.; Chmelickova, H.; Nozka, L.; Moudry, J. Non-destructive Real Time Monitoring of the Laser Welding Process. *J. Mater. Eng. Perform.* **2012**, *21*, 764–769. https://doi.org/10.1007/s11665-012-0193-4.
53. Sibillano, T.; Rizzi, D.; Mezzapesa, F.P.; Lugarà, P.M.; Konuk, A.R.; Aarts, R.; Veld, B.H.I..; Ancona, A. Closed Loop Control of Penetration Depth during CO_2 Laser Lap Welding Processes. *Sensors* **2012**, *12*, 11077–11090. https://doi.org/10.3390/s120811077.
54. Smurov, I. Pyrometry applications in laser machining. *Laser-Assist. Microtechnol.* **2001**, *4157*, 55–67. https://doi.org/10.1117/12.413774.
55. Bertrand, P.; Smurov, I.; Grevey, D. Application of near infrared pyrometry for continuous Nd:YAG laser welding of stainless steel. *Appl. Surf. Sci.* **2000**, *168*, 182–185. https://doi.org/10.1016/s0169-4332(00)00586-9.
56. Farson, D.; Ali, A.; Sang, Y. Relationship of optical and acoustic emissions to laser weld penetration. *Weld. J.* **1998**, *77*, 142-s.
57. Kamimuki, K.; Inoue, T.; Yasuda, K.; Muro, M.; Nakabayashi, T.; Matsunawa, A. Behaviour of monitoring signals during detection of welding defects in YAG laser welding. Study of monitoring technology for YAG laser welding (Report 2). *Weld. Int.* **2003**, *17*, 203–210.
58. Smurov, I. Laser process optical sensing and control. In Proceedings of the IV International WLT-Conference on Lasers in Manufacturing, Munich, Germany, 18–22 June 2007; pp. 537–546.
59. Chu, T.C.; Ranson, W.F.; Sutton, M.A. Applications of digital-image-correlation techniques to experimental mechanics. *Exp. Mech.* **1985**, *25*, 232–244. https://doi.org/10.1007/bf02325092.
60. Chao, Y.J.; Luo, P.-F.; Sutton, M.A. Application of stereo vision to three-dimensional deformation analyses in fracture experiments. *Opt. Eng.* **1994**, *33*, 981–990. https://doi.org/10.1117/12.160877.

61. Peters, W.H.; Ranson, W.F. Digital Imaging Techniques in Experimental Stress Analysis. *Opt. Eng.* **1982**, *21*, 213427. https://doi.org/10.1117/12.7972925.
62. Lightfoot, M. The measurement of welding distortion in shipbuilding using close range photogrammetry. In Proceedings of the Remote Sensing and Photogrammetry Society, Newcastle upon Tyne, UK, 11–14 September 2007.
63. Dye, D.; Hunziker, O.; Roberts, S.M.; Reed, R.C. Modeling of the mechanical effects induced by the tungsten inert-gas welding of the IN718 superalloy. *Met. Mater. Trans. A* **2001**, *32*, 1713–1725. https://doi.org/10.1007/s11661-001-0149-z.
64. Masubuchi, K. *CHAPTER 3-Fundamental Information on Residual Stresses Analysis of Welded Structures;* Pergamon: Oxford, UK, 1980.
65. Salzburger, H.J.; Mohrbacher, H.; Kralj, S.; Kozuh, Z. In-line quality control of laser welds of tailored blanks by couplant free ultrasonic inspection. In Proceedings of the European Federation for Non-Destructive Testing (EFNDT), European Conference on Nondestructive Testing, Barcelona, Spain, 17–21 June 2002.
66. Nakamura, S.; Sakurai, M.; Kamimuki, K.; Inoue, T.; Ito, Y. Detection technique for transition between deep penetration mode and shallow penetration mode in CO_2laser welding of metals. *J. Phys. D Appl. Phys.* **2000**, *33*, 2941–2948. https://doi.org/10.1088/0022-3727/33/22/311.
67. Passini, A.; de Oliveira, A.C.; Riva, R.; Travessa, D.N.; Cardoso, K.R. Ultrasonic inspection of AA6013 laser welded joints. *Mater. Res.* **2011**, *14*, 417–422. https://doi.org/10.1590/s1516-14392011005000057.
68. Mai, T.A.; Spowage, A.C. Characterisation of dissimilar joints in laser welding of steel–kovar, copper–steel and copper–aluminium. *Mater. Sci. Eng. A* **2004**, *374*, 224–233.
69. Miller, M.; Mi, B.; Kita, A.; Ume, I. Development of automated real-time data acquisition system for robotic weld quality monitoring. *Mechatronics* **2002**, *12*, 1259–1269. https://doi.org/10.1016/s0957-4158(02)00028-4.
70. Zhang, X.-G.; Xu, J.-J.; Ge, G.-Y. Defects recognition on X-ray images for weld inspection using SVM. In Proceedings of the Proceedings of the 2004 International Conference on Machine Learning and Cybernetics (IEEE Cat. No. 04EX826), Shanghai, China, 26–29 August 2004; IEEE: Manhattan, NY, USA, 2004; volume 6, pp. 3721–3725.
71. Colegrove, P.; Ikeagu, C.; Thistlethwaite, A.; Williams, S.; Nagy, T.; Suder, W.; Steuwer, A.; Pirling, T. Welding process impact on residual stress and distortion. *Sci. Technol. Weld. Join.* **2009**, *14*, 717–725. https://doi.org/10.1179/136217109x406938.
72. Chao, Y.J.; Zhu, X.; Qi, X. 'WELDSIM-A WELDing SIMulation code for the determination of transient and residual temperature, stress, and distortion. *Adv. Comput. Eng. Sci.* **2000**, *2*, 1207–1211.
73. Zösch, A.; Seidel, M.; Qualitätssicherung, I.I.F.M. Non destructive testing of laser welded lap seams by eddy current technique. In 9th European Conference on NDT-ECNDT 2006, Berlin, Germany, September 2006. Available online: https://www.ndt.net/article/ecndt2006/doc/P99.pdf (accessed on 17 June 2022).
74. Todorov, E.; Nagy, B.; Levesque, S.; Ames, N.; Na, J. Inspection of laser welds with array eddy current technique. In Proceedings of the AIP Conference Proceedings, Anchorage, AK, USA, 22–26 September 2003; American Institute of Physics: College Park, MD, USA, 2003; Volume 1511, pp. 1065–1072.
75. Lashkia, V. Defect detection in X-ray images using fuzzy reasoning. *Image Vis. Comput.* **2001**, *19*, 261–269. https://doi.org/10.1016/s0262-8856(00)00075-5.
76. Ho, S.K.; White, R.M.; Lucas, J. A vision system for automated crack detection in welds. *Meas. Sci. Technol.* **1990**, *1*, 287–294. https://doi.org/10.1088/0957-0233/1/3/015.
77. Ma, N.; Gao, X.; Wang, C.; Zhang, Y. Optimization of Magneto-Optical Imaging Visualization of Micro-Defects Under Combined Magnetic Field Based on Dynamic Permeability. *IEEE Trans. Instrum. Meas.* **2021**, *70*, 1–9. https://doi.org/10.1109/tim.2021.3117074.
78. Radtke, U.; Zielke, R.; Rademacher, H.G.; Crostack, H.A.; Hergt, R. Application of magneto-optical method for real-time visualization of eddy currents with high spatial resolution for nondestructive testing. *Opt. Lasers Eng.* **2001**, *36*, 251–268.
79. Gao, X.; Lan, C.; You, D.; Li, G.; Zhang, N. Weldment Nondestructive Testing Using Magneto-optical Imaging Induced by Alternating Magnetic Field. *J. Nondestruct. Eval.* **2017**, *36*, 55. https://doi.org/10.1007/s10921-017-0434-4.
80. Ma, N.; Gao, X.; Tian, M.; Wang, C.; Zhang, Y.; Gao, P.P. Magneto-Optical Imaging of Arbitrarily Distributed Defects in Welds under Combined Magnetic Field. *Metals* **2022**, *12*, 1055. https://doi.org/10.3390/ met12061055.
81. Li, Y.; Gao, X.; Zheng, Q.; Gao, P.P.; Zhang, N. Weld cracks nondestructive testing based on magneto-optical imaging under alternating magnetic field excitation. *Sensors Actuators A Phys.* **2018**, *285*, 289–299. https://doi.org/10.1016/j.sna.2018.11.017.
82. Nayak, S.S.; Biro, E.; Zhou, Y. *Laser Welding of Advanced High-Strength Steels (AHSS)*; Elsevier Ltd.: Amsterdam, The Netherlands, 2015; ISBN 9780857098580.
83. Pereira, A.B.; Santos, R.O.; Carvalho, B.S.; Butuc, M.C.; Vincze, G.; Moreira, L.P. The Evaluation of Laser Weldability of the Third-Generation Advanced High Strength Steel. *Metals* **2019**, *9*, 1051. https://doi.org/10.3390/met9101051.
84. Oliveira, D.F. *Pârametros da Soldadura LASER Pulsado de Nd:YAG em Aços Avançados de Alta Resistência*; University of Aveiro: Aveiro, Portugal, 2015.
85. Farabi, N.; Chen, D.; Zhou, Y. Fatigue properties of laser welded dual-phase steel joints. *Procedia Eng.* **2010**, *2*, 835–843. https://doi.org/10.1016/j.proeng.2010.03.090.
86. Xie, C.; Yang, S.; Liu, H.; Zhang, Q.; Cao, Y.; Wang, Y. Microstructure and Fatigue Properties of Laser Welded DP590 Dual-Phase Steel Joints. *J. Mater. Eng. Perform.* **2017**, *26*, 3794–3801. https://doi.org/10.1007/s11665-017-2848-7.
87. Sun, Q.; Di, H.-S.; Li, J.; Wang, X.-N. Effect of pulse frequency on microstructure and properties of welded joints for dual phase steel by pulsed laser welding. *Mater. Des.* **2016**, *105*, 201–211. https://doi.org/10.1016/j.matdes.2016.05.071.

88. Mansur, V.M.; Mansur, R.A.D.F.; de Carvalho, S.M.; de Siqueira, R.H.M.; de Lima, M.S.F. Effect of laser welding on microstructure and mechanical behaviour of dual phase 600 steel sheets. *Heliyon* **2021**, *7*, e08601. https://doi.org/10.1016/j.heliyon.2021.e08601.
89. Tunçel, O.; Aydın, H.; Çetin, Ş. Microstructure and Mechanical Properties of Similar and Dissimilar Laser Welds of DP600 and DP1000 Steel Sheets Used in the Automotive Industry. *Turk. J. Eng.* **2020**, *5*, 8–14. https://doi.org/10.31127/tuje.649975.
90. Gandhi, A.; Kundu, A.; Sarkar, A.; Mahato, J.K.; Chakraborti, P.C. Effect of Laser Pulse Duration on Tensile and Electrochemical Behavior of Laser-Welded Dual-Phase Steel. *J. Mater. Eng. Perform.* **2021**, *30*, 4263–4281. https://doi.org/10.1007/s11665-021-05715-2.
91. Huang, T.; Xin, L.J.; Wang, Z.Y. Study on Fiber Laser Welding for DP780 High Strength Steel. *Adv. Mater. Res.* **2011**, *328–330*, 48–53. https://doi.org/10.4028/www.scientific.net/amr.328-330.48.
92. Jia, Q.; Guo, W.; Peng, P.; Li, M.; Zhu, Y.; Zou, G. Microstructure- and Strain Rate-Dependent Tensile Behavior of Fiber Laser-Welded DP980 Steel Joint. *J. Mater. Eng. Perform.* **2016**, *25*, 668–676. https://doi.org/10.1007/s11665-015-1864-8.
93. Parkes, D.; Xu, W.; Westerbaan, D.; Nayak, S.; Zhou, Y.; Goodwin, F.; Bhole, S.; Chen, D. Microstructure and fatigue properties of fiber laser welded dissimilar joints between high strength low alloy and dual-phase steels. *Mater. Des.* **2013**, *51*, 665–675. https://doi.org/10.1016/j.matdes.2013.04.076.
94. Saha, D.; Westerbaan, D.; Nayak, S.; Biro, E.; Gerlich, A.; Zhou, Y. Microstructure-properties correlation in fiber laser welding of dual-phase and HSLA steels. *Mater. Sci. Eng. A* **2014**, *607*, 445–453. https://doi.org/10.1016/j.msea.2014.04.034.
95. Xu, W.; Westerbaan, D.; Nayak, S.; Chen, D.; Goodwin, F.; Biro, E.; Zhou, Y. Microstructure and fatigue performance of single and multiple linear fiber laser welded DP980 dual-phase steel. *Mater. Sci. Eng. A* **2012**, *553*, 51–58. https://doi.org/10.1016/j.msea.2012.05.091.
96. Wan, Z.; Guo, W.; Jia, Q.; Xu, L.; Peng, P. Hardness Evolution and High Temperature Mechanical Properties of Laser Welded DP980 Steel Joints. *High Temp. Mater. Process.* **2017**, *37*, 587–595. https://doi.org/10.1515/htmp-2017-0007.
97. Zhao, Y.Y.; Zhang, Y.S.; Hu, W. Effect of welding speed on microstructure, hardness and tensile properties in laser welding of advanced high strength steel. *Sci. Technol. Weld. Join.* **2013**, *18*, 581–590. https://doi.org/10.1179/1362171813y.0000000140.
98. Ferreira, C.C.D.A.; Braga, V.; de Siqueira, R.H.M.; de Carvalho, S.M.; de Lima, M.S.F. Laser beam welding of DP980 dual phase steel at high temperatures. *Opt. Laser Technol.* **2020**, *124*, 105964. https://doi.org/10.1016/j.optlastec.2019.105964.
99. Sisodia, R.P.S.; Gáspár, M. Investigation of Metallurgical and Mechanical Properties of Laser Beam Welded and Post-weld Heat Treated DP1400 Steel. *J. Mater. Eng. Perform.* **2021**, *30*, 1703–1710. https://doi.org/10.1007/s11665-021-05469-x.
100. Chen, X.; Niu, C.; Lian, C.; Lin, J. The Evaluation of Formability of the 3rd Generation Advanced High Strength Steels QP980 based on Digital Image Correlation Method. *Procedia Eng.* **2017**, *207*, 556–561. https://doi.org/10.1016/j.proeng.2017.10.1020.
101. Di, H.; Sun, Q.; Wang, X.; Li, J. Microstructure and properties in dissimilar/similar weld joints between DP780 and DP980 steels processed by fiber laser welding. *J. Mater. Sci. Technol.* **2017**, *33*, 1561–1571. https://doi.org/10.1016/j.jmst.2017.09.001.
102. Bandyopadhyay, K.; Lee, M.-G.; Panda, S.K.; Saha, P.; Lee, J. Formability assessment and failure prediction of laser welded dual phase steel blanks using anisotropic plastic properties. *Int. J. Mech. Sci.* **2017**, *126*, 203–221. https://doi.org/10.1016/j.ijmecsci.2017.03.022.
103. Alves, P.; Lima, M.; Raabe, D.; Sandim, H. Laser beam welding of dual-phase DP1000 steel. *J. Mater. Process. Technol.* **2017**, *252*, 498–510. https://doi.org/10.1016/j.jmatprotec.2017.10.008.
104. Wang, X.-N.; Sun, Q.; Zheng, Z.; Di, H.-S. Microstructure and fracture behavior of laser welded joints of DP steels with different heat inputs. *Mater. Sci. Eng. A* **2017**, *699*, 18–25. https://doi.org/10.1016/j.msea.2017.05.078.
105. He, H.; Forouzan, F.; Volpp, J.; Robertson, S.; Vuorinen, E. Microstructure and Mechanical Properties of Laser-Welded DP Steels Used in the Automotive Industry. *Materials* **2021**, *14*, 456. https://doi.org/10.3390/ma14020456.
106. *ISO 3834-1:2005*; Quality Requirements for Fusion Welding of Metallic Materials—Part 1: Criteria for the Selection of the Appropriate Level of Quality Requirements. International Organization for Standardization: Geneva, Switzerland, 2005.
107. *ISO 3834-2:2005*; Quality Requirements for Fusion Welding of Metallic Materials—Part 2: Comprehensive Quality Requirements. International Organization for Standardization: Geneva, Switzerland, 2005.
108. *ISO 3834-4:2005*; Quality Requirements for Fusion Welding of Metallic Materials—Part 4: Elementary Quality Requirements. International Organization for Standardization: Geneva, Switzerland, 2005.
109. *ISO 3834-5:2015*; Quality Requirements for Fusion Welding of Metallic Materials—Part 5: Documents with which it Is Necessary to Conform to Claim Conformity to the Quality Requirements of ISO 3834-2, ISO 3834-3 or ISO 3834-4. International Organization for Standardization: Geneva, Switzerland, 2015.
110. *ISO 9001:2015*; Quality Management Systems—Requirements; International Organization for Standardization: Geneva, Switzerland, 2015. 13. ISO. 14731:2019—Welding Coordination—Tasks and Responsibilities. International Organization for Standardization: Geneva, Switzerland, 2019.
111. *DIN 18800-7:2008*; Steel Structures—Part 7: Execution and Constructor's Qualification. German Institute for Standardization: Berlin, Germany, 2008.
112. *ISO 15609-4:2009*; Specification and Qualification of Welding Procedures for Metallic Materials—Welding Procedure Specification—Part 4: Laser Beam Welding. International Organization for Standardization: Geneva, Switzerland, 2009.